

# Partial Camera Obstruction Detection Using Single Value Image Metrics and Data Augmentation

Felipe A. Costa de Oliveira\*, Arto Niemi\*, Alberto García-Ortiz†, Frank Sill Torres\*

\*Institute for the Protection of Maritime Infrastructures (MI)

German Aerospace Center (DLR), Bremerhaven, Germany

Email: felipe.costadeoliveira@dlr.de

†Institute of Electrodynamics and Microelectronics

University of Bremen, Bremen, Germany

Email: agarcia@item.uni-bremen.de

**Abstract**—To improve the resilience and ensure the dependability of a critical system, the measurements and the derived intelligence provided by the sensors monitoring the system need to be reliable. This is increasingly challenging. As the computer vision methods evolve, the usage of cameras as a part of monitoring solutions has increased, and, consequently, the need for reliable diagnosis strategies for those image-based sensors. This work investigates the suitability of various single-value image metrics, derived from first and second-order statistics, for detecting partial camera obstruction. The presented methodology includes using data augmentation techniques to expand a small dataset of labeled images, and a score-based selection of the best metrics for the target application. The results show that even simple first-order statistics, such as the image histogram skewness, can provide good detection results. The strategy presented could be extended and adapted for the detection of other types of physical anomalies, being particularly useful for integrity assessment in applications with limited computational resources.

**Index Terms**—Camera diagnosis, image processing, integrity monitoring, fault detection, data augmentation, information reliability.

## I. INTRODUCTION

In the past few decades, the advancement of the computer vision field, with sophisticated image processing techniques and increasingly accurate machine learning (ML) based solutions, has fostered the use of cameras in sensor systems for various applications. As the state-of-the-art algorithms for image processing are reaching, and sometime surpassing, the level of human visual pattern recognition [1], new possibilities for camera based monitoring arises. However, as our reliance on these systems increases, in particular for safety critical applications such as autonomous vehicles and monitoring of strategic infrastructure, the integrity assessment of the gathered sensor information becomes indispensable. Although there has been significant research on the field of sensor integrity monitoring [2], most of the techniques focus on navigation systems, as the advancements in the field were traditionally made for the aviation sector [3]. Typically, the integrity monitoring approach relies on statistical analysis, applying a suitable model to derive an estimation for the monitored sensor parameters, followed by constructing a test statistic from the

obtained error that can be used for a hypothesis test. That approach is not directly applicable for assessing the integrity of camera based monitoring systems. However, the underlying concept of a fault detection based on hypothesis testing could be used, relying on specific image metrics as the test statistic.

Despite the enormous advancements in the computer vision capabilities, that were leveraged by the increased computational power and deep learning algorithms, there are still several open topics in the research of camera based sensor integrity. As discussed in [4], for the image processing community, the concept of image integrity is often related to authentication, meaning that the content of an image has not been altered in a malicious or unintended way. The methods to assess and ensure integrity are typically relying on the detection of digital image artifacts and cryptographic signature protection measures. In the context of a camera based monitoring system, these methods would be useful for detecting and preventing image manipulation attacks, in case there is a security breach on the access of the monitoring data. However, in case of physical anomalies, such as the ones derived from changes in the environmental conditions, the integrity assessment strategy would have to be different. For that case, there have been several studies on camera tampering detection [5], [6], with methods to identify obstruction or an unintended change in the camera position. These methods, usually based on edge detection [7], are employed for surveillance cameras and require a static or known background plane, being unsuitable for situations where the scenery is dynamic or unknown. To deal with that scenario, methods such as soiling detection and visibility restoration for cameras in autonomous vehicles could be used [8]. Additionally, there have been studies on visibility enhancement and de-weathering methods for improving the quality of images under bad weather conditions [9]. However, the methods found in the literature are insufficient to cover all possible scenarios of physical anomalies that can impact the reliability of a camera based monitoring system. Therefore, the development of new solutions and the investigation of different approaches for that problem are still desirable.

Building upon that scenario, this work investigates the detection of partial camera obstruction using various first

This work was funded by a doctorate scholarship provided by the Deutscher Akademischer Austauschdienst (DAAD), number 57540125.

and second order image statistics. In contrast to the tampering detection techniques used for surveillance cameras, the proposed approach can be used for single images with unknown or dynamic background and for applications with limited computational resources. Our methodology relies on applying a data based diagnosis and health monitoring strategy to camera systems, using single value image statistics as inputs, and the selection of the best metrics using feature engineering concepts. The results, derived from a small dataset of images that was expanded using data augmentation techniques, outlines the performance of various image metrics for the detection of partial camera obstruction. The metrics were evaluated as individual test statistics, and also, used as features for two ML based classifiers. Although the obtained results are specific for a particular dataset and scenario, the proposed methodology can be extended to detect physical anomalies in camera based monitoring systems in various applications.

## II. METHODOLOGY

### A. Diagnosis and Health Monitoring of Camera Systems

Prognosis and Health Management (PHM) solutions assist in the prediction of faults of components and processes, perform diagnostics of the current operational condition, and provide guidance for preventive or corrective maintenance [10]. The data provided by the monitoring system is often processed automatically by algorithms that extracts the necessary information for a particular application. The PHM concept is usually applied for Remaining Useful Life (RUL) estimation and optimized predictive maintenance in systems where component failure and degradation are an issue. That approach usually follows a four-step framework consisting of data acquisition, diagnostics, prognostics and health management [10].

The prognostics usually relies on a degradation model of key components in order to make prediction of faults and RUL. The health management aspect includes the decision-making process of maintenance actions. The data acquisition, containing appropriate data processing and conditioning steps, and the diagnosis, that relies on monitoring the target system with a suitable fault detection strategy, are directly applicable to the scenario discussed in this work. Therefore, some methods used in PHM could be used for camera based monitoring systems, in particular for the detection of physical defects that compromise the provided information, and for deriving actionable measures to restore the monitoring solution.

The problem of partial camera obstruction can be viewed as a type of fault for which the diagnosis of the camera system itself would be able to detect. In this sense, an unexpected physical anomaly or a change in the environmental conditions that can impair the provided information are a kind of integrity issue. Considering complex technical systems where the camera has an important monitoring role, the reliability of its provided information could have significant impacts in the whole system. Therefore, using a suitable strategy to evaluate the information integrity can be necessary.

The automated detection of these types of faults prompts a warning that the provided information might not be reliable, and also triggers a human intervention to do corrective maintenance in the camera to solve the issue. When that problem is seen as a type of fault, the fault detection strategies that have been fully investigated and proven in the diagnosis, reliability, health monitoring and other related fields can be used [11], [12].

Although there are a lot of different fault detection methods and strategies, suitable for different applications, a simple approach would be to investigate the distribution of image parameters under the normal and faulty conditions. If for a given parameter there is a significant difference between those distributions, that parameter is a good metric to use for the detection. In this context, a discussion of suitable image metrics for the detection of physical anomalies will be presented. The selection and evaluation of the image metrics follows a feature engineering methodology such as the one outlined in [13].

### B. Image Analysis Metrics

There are several metrics, or statistics, computed from the pixel levels of an image that can provide useful insights about the characteristics of the captured scene. The most common metrics are the so-called first and second order statistics. These metrics have been used for image analysis in many works, such as the fog detection method described in [14] and the classification of medical images in [15].

The first order statistics, also referred as histogram properties, only accounts for the values of the pixel levels, disregarding its relative position. In this way, they consider only single pixel values, being unable to distinguish two images with the same pixels but in scrambled or different positions. On the other hand, the second order statistics takes into account the way the pixel levels are distributed, with the values derived from relationships between a pair of pixels at the time. They are often used to characterize textures [16], defining aspects such as coarseness, smoothness or pattern irregularities.

The histogram  $H(i)$  of an image contains the frequency of occurrence of a gray level  $i$  in that image. It represents the frequency of all possible gray levels  $p$ , and it is calculated by the sum of pixels with a specific value  $i$ , divided by the total number of pixels. In this way, the main first order statistics can be computed from the image histogram using the following equations:

$$\mu = \sum_{i=0}^{p-1} i H(i) \quad (1)$$

$$\mu_k = \sum_{i=0}^{p-1} (i - \mu)^k H(i) \text{ for } k = 2, 3 \text{ or } 4 \quad (2)$$

The mean  $\mu$  represents the mean brightness level of the image; the variance  $\mu_2$  is a measure of how much the values deviate from the mean; the skewness  $\mu_3$  represents the asymmetry of the histogram; and the kurtosis  $\mu_4$  can be viewed as

a measure of the sharpness of the peak around the mean value in the histogram.

The second order statistics of an image are usually represented by the Gray Level Co-occurrence Matrix (GLCM). The matrix computes the relative frequency of pairs of pixels, separated by an offset distance of  $d$  pixels following the direction of an angle  $\theta$ . Its size is defined by the number of possible pixel values, being  $256 \times 256$  for standard compressed images. In this way, an element  $P_{i,j}$  of the matrix represents how often the pixels of value  $i$  and  $j$  appear together in neighboring offset elements of distance  $d$  at an angle  $\theta$ . The angles are typically parameterized in horizontal, vertical and diagonal (0, 90 and 45 degrees), but the choice of the offset distance can depend on the types of textures and patterns, being usually set as a range of values to capture that variability of elements.

One GLCM matrix is defined for each distance and angle pair, but there are various features, which are single value metrics, that can be extracted from it. In the first work where the GLCM was presented [16], a set of 14 features were defined. Each feature represents specific characteristics of the matrix that can be related to certain texture attributes, or image patterns. However, the most used features are the Angular Second Moment (ASM), Contrast, Correlation, Homogeneity, Dissimilarity and Entropy, which can be calculated as follows:

$$Contrast = \sum_{i,j=0}^{p-1} (i-j)^2 P_{i,j} \quad (3)$$

$$Dissimilarity = \sum_{i,j=0}^{p-1} |i-j| P_{i,j} \quad (4)$$

$$ASM = \sum_{i,j=0}^{p-1} P_{i,j}^2 \quad (5)$$

$$Homogeneity = \sum_{i,j=0}^{p-1} \frac{P_{i,j}}{1+(i-j)^2} \quad (6)$$

$$Correlation = \sum_{i,j=0}^{p-1} P_{i,j} \frac{(i-\mu_x)(j-\mu_y)}{\sigma_x \sigma_y} \quad (7)$$

$$Entropy = \sum_{i,j=0}^{p-1} -P_{i,j} \log(P_{i,j}) \quad (8)$$

Where  $\mu_x, \mu_y$  and  $\sigma_x, \sigma_y$  are respectively the mean and standard deviation of the horizontal and vertical components of the matrix.

The four first order statistics and the six GLCM features presented will be evaluated in this work as metrics for partial camera obstruction detection. However, since the GLCM features are associated to an offset distance and angle, to avoid having an excessive number of parameters, a strategy to summarize those values was developed.

The optimal distance that maximizes the differences in the values for the different types of images that are being classified depends on the patterns in the textures of the images. Since for

Example of GLCM Derived Metrics

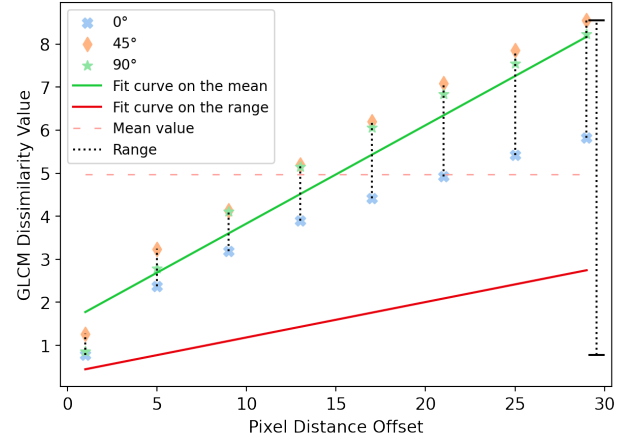


Fig. 1. Example of the derived GLCM metrics for the dissimilarity parameter.

an arbitrary scene that is unknown, a range of offset distances between 1 and 32 pixels (as proposed in [17]) was chosen and metrics derived from those values were used. These metrics are, the mean value and range (the difference between the maximum and minimum value) of the GLCM feature for all distances and angles, and the first order fitted slope of the values in respect to the offset distance. In this way, there would be three values for each feature, and for each angle. To account for the variability between different angles, a first order slope for that range of values was also included. Therefore, for each GLCM feature there are four metrics being considered, instead of one for each pair of distance and angle. The plot in Fig. 1 shows an example of those summarized metrics for the dissimilarity feature.

### C. Image Data Augmentation Techniques

One of the main issues in data based classification problems is the acquisition of sufficient labeled data. In the context of this work, the challenge would be creating a balanced dataset of images in different scenarios and conditions with and without partial camera obstruction. Instead of resorting to such a costly and time-consuming data gathering campaign, the use of data augmentation techniques in a small dataset of reference images could be an effective solution. The main strategy consists of applying various types of image transformations in a randomized way, generating an arbitrarily large amount of different images that are based on the same source. The drawback is that the expanded dataset would still be limited to some underlying characteristics of the original dataset, with extended variability around that original source. Some simple, yet effective, data augmentation techniques are the following [18]:

- Geometrical transformations, such as change in the perspective (skew and shear), rotation, mirroring (horizontal and vertical flip);
- Color, brightness, contrast and sharpness adjustments;

- Cropping and zooming, which selects a smaller region of the image;
- Erasing, the replacement of parts of the image with random noise.

Other strategies, that are based on ML, are texture and style transfer [19], and synthetic images created by Generative Adversarial Networks (GAN) [20], [21], [22]. However, in this work, only the geometrical transformations, random cropping, brightness, contrast and sharpness adjustments will be used.

### III. EXPERIMENTS AND RESULTS

#### A. Framework for Image Data Augmentation

A framework for testing integrity assessment methods for camera based monitoring systems was developed. The goal was to have a tool able to simulate the output of a monitoring system, that could be comprised of several image based sensors, under different conditions and scenarios. The software works by selecting an image, from a dataset of reference images, that matches a specific user defined job configuration. Then, it can apply image transformations (data augmentation techniques), in a randomized manner or according to a desired input. Additionally, the framework is capable of introducing artificially generated defects, but that functionality will not be covered in this work. The software was developed in Python following an Object-Oriented Programming (OOP) paradigm and using popular open source image processing libraries, such as Python Image Library (PIL), Scikit-image and OpenCV. The diagram in Fig. 3 shows the data-flow and outlines the features of the framework.

The proposed framework can assist on the evaluation and development of integrity assessment methods, with the goal of improving the reliability of the monitoring solution. In this way, the software was used to extend on an existing dataset of natural images with and without partial camera obstruction. The original images were taken with different exposure times from a single scenario, under normal conditions and with two different instances of obstruction, as depicted in Fig. 4. The camera used was a Teledyne E2V Bora 1.3Mp [23], which contains a Time-of-Flight (ToF) specialized image sensor suitable for machine vision applications. The original dataset was expanded to a balanced set of 4000 images using the data augmentation techniques described in the section II-C. A special care with the random crop parameters was made for the images with partial camera obstruction, to avoid cropping into a region containing only the obstruction profile. The Fig. 2 shows examples of the produced images for the non-obstructed scenario.

#### B. Image Metrics Selection

The image metrics discussed in II-B were computed for the original and augmented dataset. The developed framework enabled extending the variability of the analyzed image parameters without performing further data gathering campaigns. The combined distribution and scatter plots in figure 5 show the relationship and variation of four of the selected image parameters under the normal, and partially obstructed scene.

The metrics were ranked based on a score calculated from the difference of the mean values divided by the sum of the standard deviation for the normalized values (scaling between 0 and 1) in each of the two categories. In this way, the score, called here M-Score for the sake of differentiating it, is a measure of the separability between the distributions, favoring the metrics with the smallest overlap in their histograms. Additionally, the Kullback-Leibler divergence [24] and the Bhattacharyya distance [25] were also considered. Those are measures of the similarity between two statistical distributions. However, the image metrics selected using these quantities had a worse performance when used as the features for the detection of the partial obstruction defect. Therefore, the simple M-Score related to the difference between the means was used for the selection of the best metrics.

TABLE I: Selected image metrics and their score for partial obstruction detection.

Image Metric	M-Score	F1-Score
Skew	1.178	0.934
GLCM Correlation Fit Slope Mean	1.169	0.900
GLCM Homogeneity Mean	1.144	0.878
GLCM Dissimilarity Range	1.121	0.877
GLCM Dissimilarity Fit Slope Mean	1.102	0.867
GLCM Dissimilarity Mean	1.090	0.862
GLCM Contrast Range	1.057	0.864
Mean Brightness Level	1.048	0.817
GLCM Correlation Range	1.046	0.892
GLCM Contrast Fit Slope Mean	1.040	0.853

#### C. Partial Camera Obstruction Detection

Simple detection tests in which each individual metric is used as a test statistic were conducted. The optimal threshold for each metric was determined by performing a Kolmogorov-Smirnov test of goodness of fit for a range of possible values for the metric of interest, in respect to the distributions of the null and alternative hypothesis (normal and partially obstructed conditions). Performing the test in a range of values and extracting the p-value lines from both conditions enables the optimal selection of the threshold value, being the intersection between the two p-value lines, as shown in figure 6. In the design of a statistical test there is always a compromise between false positives and false negatives (type I and II errors). Therefore, the selection of the threshold value can be tailored to prioritize the avoidance of either one of these errors, but not both at the same time. The optimal value considered in this work is the one that balances those two errors, providing the best average detection rate between the two categories. Note that in some cases, for bad metrics, the overlap between the two distributions is so large that the p-value curves does



Fig. 2. Example of applying various data augmentation techniques to a sample image: (a) - Original image; (b) - Size preserving skew; (c) - Size preserving shear; (d) - Size preserving rotation; (e) - Horizontal flip; (f) - Random crop; (g) - Contrast increase; (h) - All combined.

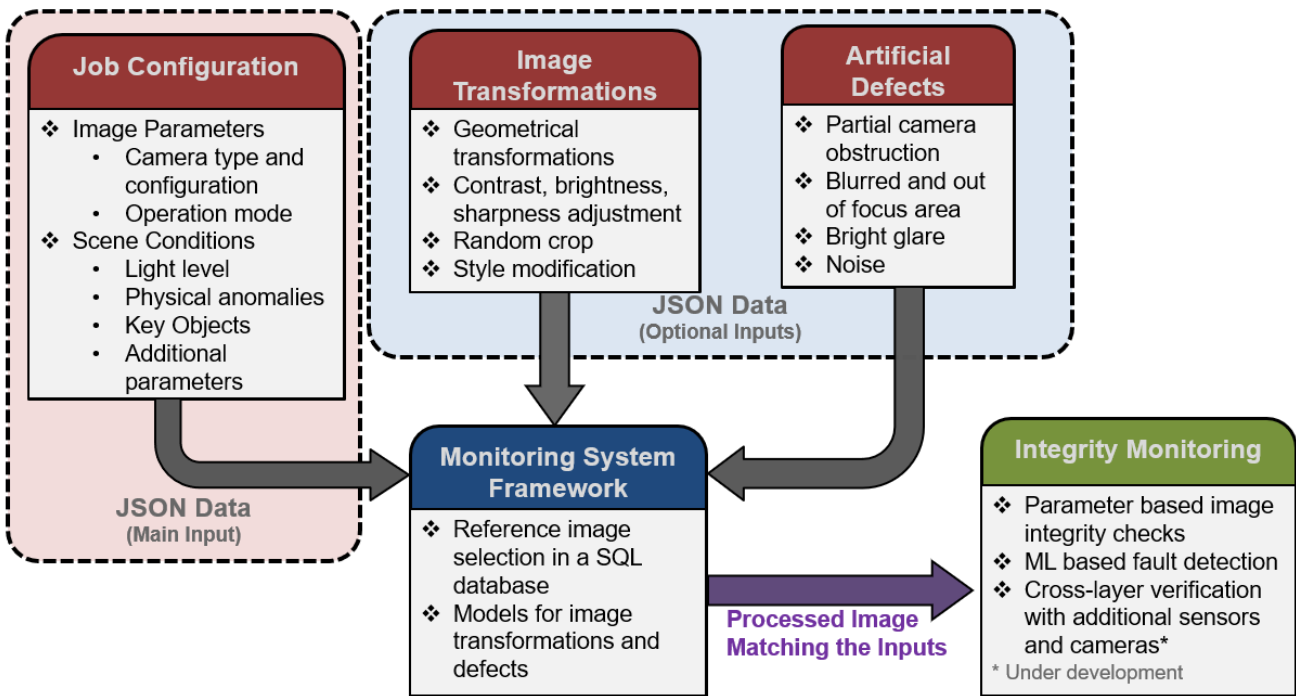


Fig. 3. Representation of the proposed monitoring system framework, outlining the data-flow and its features.



Fig. 4. Sample of the original dataset: (a) - Normal scene; (b) and (c) - Partially obstructed camera.

not intercepted. Those metrics were removed from consideration. Alternatively, the threshold value could be determined from the intersection of the Kernel Density Estimation curves, which gave very similar results.

These tests based on a single metric were conducted using the extended dataset of images and the detection result was evaluated in terms of the weighted average F1 score, which considers the precision and recall for the detection of the two categories (normal and partially obstructed). The obtained F1-score showed high correlation with the M-Score previously

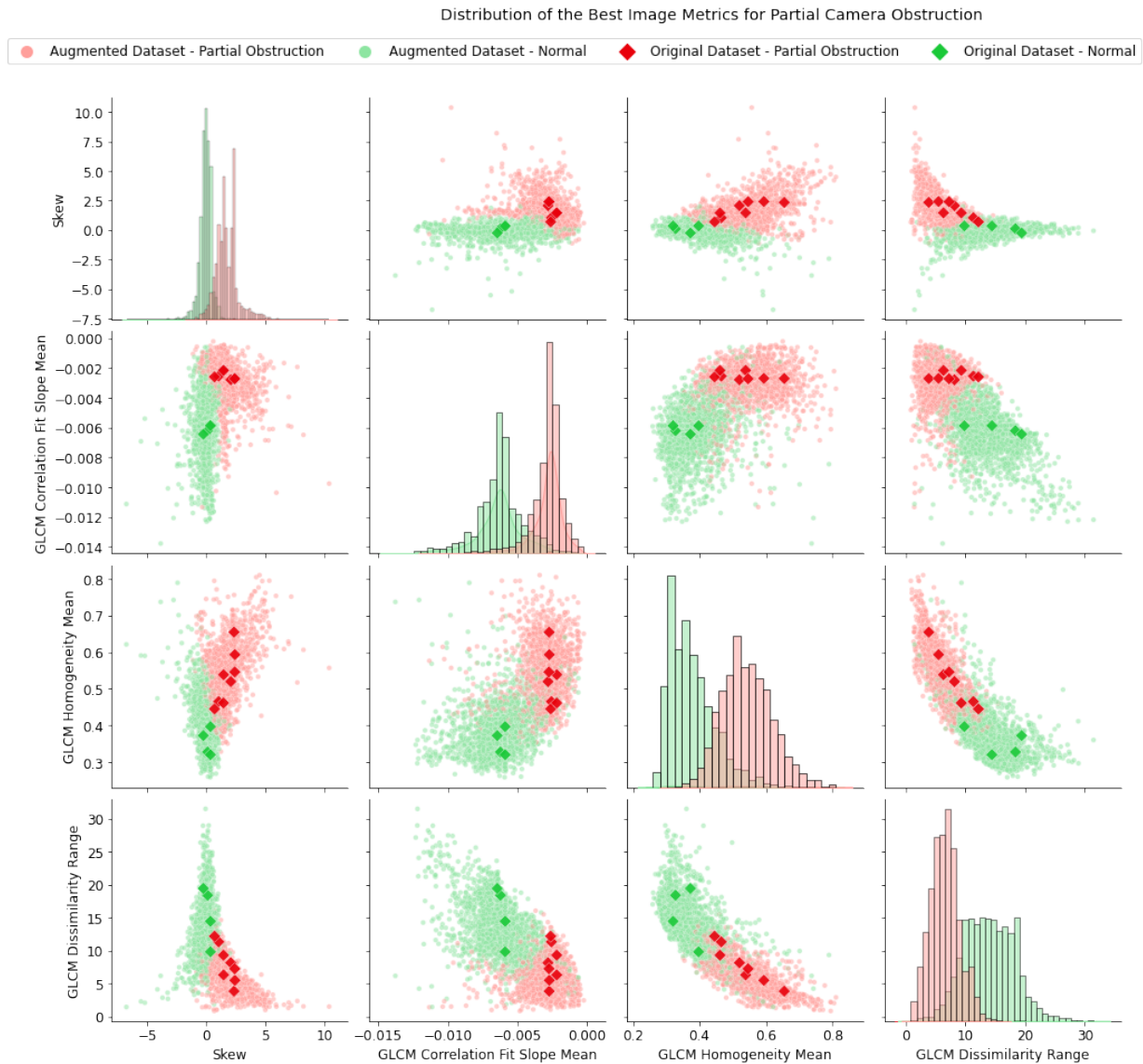


Fig. 5. Variation of the image metrics that had the highest score for the detection of partial camera obstruction.

discussed. The results for the best metrics are presented in table I.

In addition to the tests based on an individual metric, two types of ML classifiers, an Artificial Neural Network (ANN) and a Random Forest algorithm, were trained following an 80-20 train-validation split using the 10 best image metrics presented as features. Since the train-validation split is randomized, the performance of the ML classifiers were evaluated over 100 runs. The F1 score of the weighted average between the two categories was used as the evaluation metric. The results were computed for the augmented dataset, containing 4000 images, and also for the original dataset, with only 12 images. As expected, the average F1 score for the augmented dataset was better, 0.883 against 0.842 for the ANN, and 0.914 against 0.812 for the Random Forest. Moreover, the distribution plots in figure 7 shows that the results were

more consistent for the augmented dataset, supporting the use of data augmentation techniques even for very small datasets. Although the classifiers trained with only the original small dataset had perfect scores sometimes, that is clearly a sign of overfitting. When using the augmented dataset as validation data for the classifiers that were trained with the small original dataset, the F1 score was very close to the average of the 100 runs, being 0.851 for the ANN and 0.824 for the Random Forest. Therefore, expanding the dataset with data augmentation techniques improved the detection rate.

#### IV. DISCUSSION AND CONCLUSION

It is surprising to note that an ML based classifier had, on average, a lower detection rate than the simple threshold based test using the best individual image metric. The average F1 score for the Random Forest classifier was 0.914, while

P-values of the Goodness of Fit Test for the Skew Metric

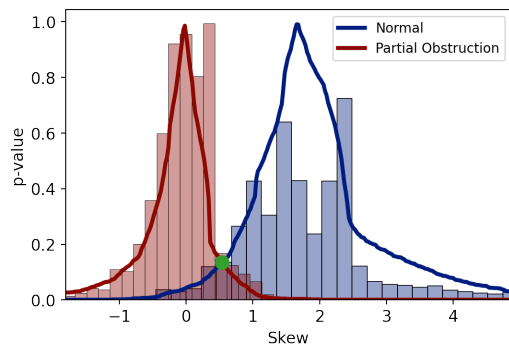


Fig. 6. Example of the threshold value determination process for the Skew metric. The curves represents the p-value of a Kolmogorov-Smirnov test of goodness of fit, performed for a range of skew values in comparison to the whole sample distribution of that parameters, in the normal and partially obstructed cases. The intersection of the curves is a good estimation for the optimal threshold value for that metric.

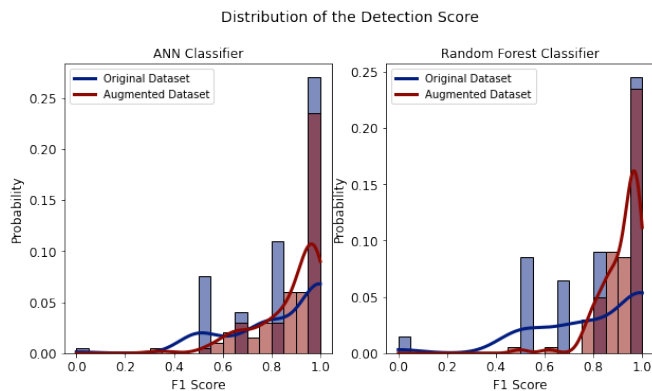


Fig. 7. Distribution of the F1 score for the detection of partial camera obstruction using two classifiers, in the augmented and original image dataset.

the same score for the Skew (histogram skewness) metric was 0.934. That can be explained by the fact that no feature selection and parameter optimization were performed for the ML based approach. Those results could probably be improved by conducting such an optimization. Nevertheless, it is remarkable that a simple approach, based on the calculation of a first order image statistic and the comparison with a fixed threshold value, could be a good solution for this detection problem.

It is important to note the these results are highly biased for the particular camera that was used and the conditions of the scenes contained in the dataset. The fault detection performance for an arbitrary scene taken with a different camera would probably be much worse. However, the same methodology can be applied to a larger set of images, taken with different cameras and scenarios, and also expanded for the detection of other types of physical defects in the images. Although the trend in image processing research has been the use of big datasets to train complex deep learning algorithms, these methods are generally computationally expensive, and the derived solutions can be very specific. Therefore, it is

important to investigate alternative solutions, that require less processing power, and that can be tailored to cover different scenarios. In this way, the usage of simple image metrics to evaluate the reliability of the information provided by cameras could be advantageous for applications with constrained processing resources. This work presents a simple, yet, effective methodology that could be applied to those scenarios.

#### ACKNOWLEDGMENT

The authors would like to thank the Deutscher Akademischer Austauschdienst (DAAD), for providing the doctorate scholarship that funded this work, and Dr. Enno Peters, with the DLR-MI institute, for conducting the image acquisition experiments that were used in this work.

#### REFERENCES

- [1] L. E. van Dyck, R. Kwitt, S. J. Denzler, and W. R. Gruber, "Comparing object recognition in humans and deep convolutional neural networks—an eye tracking study," *Frontiers in Neuroscience*, vol. 15, 2021.
- [2] F. A. Costa de Oliveira, F. S. Torres, and A. Garcia-Ortiz, "Recent advances in sensor integrity monitoring methods—a review," *IEEE Sensors Journal*, vol. 22, no. 11, pp. 10256–10279, 2022.
- [3] P. Zabalegui, G. De Miguel, A. Pérez, J. Mendizabal, J. Goya, and I. Adin, "A review of the evolution of the integrity methods applied in gnss," *IEEE Access*, vol. 8, pp. 45813–45824, 2020.
- [4] P. Korus, "Digital image integrity – a survey of protection and verification techniques," *Digital Signal Processing*, vol. 71, pp. 1–26, 2017.
- [5] S. M. Hosseini and A. H. Taherinia, "Anomaly and tampering detection of cameras by providing details," in *2016 6th International Conference on Computer and Knowledge Engineering (ICCKE)*, pp. 165–170, 2016.
- [6] A. Saglam and A. Temizel, "Real-time adaptive camera tamper detection for video surveillance," in *2009 Sixth IEEE International Conference on Advanced Video and Signal Based Surveillance*, pp. 430–435, 2009.
- [7] G.-b. Lee, Y.-c. Shin, J.-h. Park, and M.-j. Lee, "Low-complexity camera tamper detection based on edge information," in *2014 IEEE International Conference on Consumer Electronics - Taiwan*, pp. 155–156, 2014.
- [8] M. Uříčář, H. Rashed, A. Ranga, A. Dahal, and S. Yogamani, "Visibility-tynet: Camera visibility detection and image restoration for autonomous driving," in *Electronic Imaging, Autonomous Vehicles and Machines*, 07 2020.
- [9] A. C. Aponso and N. Krishnarajah, "Review on state of art image enhancement and restoration methods for a vision based driver assistance system with de-weathering," in *2011 International Conference of Soft Computing and Pattern Recognition (SoCPar)*, pp. 135–140, 2011.
- [10] R. Moradi and K. M. Groth, "Modernizing risk assessment: A systematic integration of pra and phm techniques," *Reliability Engineering & System Safety*, vol. 204, p. 107194, 2020.
- [11] A. Abid, M. T. Khan, and J. Iqbal, "A review on fault detection and diagnosis techniques: basics and beyond," *Artificial Intelligence Review*, vol. 54, pp. 3639–3664, Jun 2021.
- [12] D. Souza, M. Granzotto, G. Almeida, and L. C. Oliveira Lopes, "Fault detection and diagnosis using support vector machines –a SVC and SVR comparison," *Journal of Safety Engineering*, vol. 2014, pp. 18–29, 04 2014.
- [13] Y. Hu, X. Miao, Y. Si, E. Pan, and E. Zio, "Prognostics and health management: A review from the perspectives of design, development and decision," *Reliability Engineering & System Safety*, vol. 217, p. 108063, 2022.
- [14] R. Asery, R. K. Sunkaria, L. D. Sharma, and A. Kumar, "Fog detection using GLCM based features and svm," in *2016 Conference on Advances in Signal Processing (CASP)*, pp. 72–76, 2016.
- [15] N. Aggarwal and R. Agrawal, "First and second order statistics features for classification of magnetic resonance brain images," *Journal of Signal and Information Processing*, vol. 03, 01 2012.
- [16] R. M. Haralick, K. Shanmugam, and I. Dinstein, "Textural features for image classification," *IEEE Transactions on Systems, Man, and Cybernetics*, vol. SMC-3, no. 6, pp. 610–621, 1973.

- [17] A. Gebejes and R. Huertas, "Texture characterization based on grey-level co-occurrence matrix," *International Conference on Information and Communication Technologies*, pp. 375–378, 01 2013.
- [18] A. Mikołajczyk and M. Grochowski, "Data augmentation for improving deep learning in image classification problem," in *2018 International Interdisciplinary PhD Workshop (IIPhDW)*, pp. 117–122, 2018.
- [19] P. T. G. Jackson, A. A. Abarghouei, S. Bonner, T. P. Breckon, and B. Obara, "Style augmentation: Data augmentation via style randomization," *CoRR*, vol. abs/1809.05375, 2018.
- [20] M. Uricár, G. Sistu, H. Rashed, A. Vobecký, P. Krížek, F. Bürger, and S. K. Yogamani, "Let's get dirty: GAN based data augmentation for soiling and adverse weather classification in autonomous driving," *CoRR*, vol. abs/1912.02249, 2019.
- [21] Y. Steiniger, D. Kraus, and T. Meisen, "Generating synthetic sidescan sonar snippets using transfer-learning in generative adversarial networks," *Journal of Marine Science and Engineering*, vol. 9, no. 3, 2021.
- [22] A. Sauer, K. Schwarz, and A. Geiger, "StyleGAN-XL: Scaling StyleGAN to large diverse datasets," in *ACM SIGGRAPH*, vol. abs/2201.00273, 2022.
- [23] Teledyne, *BORA Datasheet - 1.3 Megapixels 3D Time-Of-Flight CMOS Sensor*, 11 2018.
- [24] S. Kullback and R. A. Leibler, "On Information and Sufficiency," *The Annals of Mathematical Statistics*, vol. 22, no. 1, pp. 79 – 86, 1951.
- [25] A. Bhattacharyya, "On a measure of divergence between two statistical populations defined by their probability distributions," *Bull. Calcutta Math. Soc.*, vol. 35, pp. 99–109, 1943.